ELSEVIER

Nuclear Physics A 683 (2001) 406–424

NUCLEAR PHYSICS A

www.elsevier.nl/locate/npe

Phenomenological construction of a relativistic nucleon–nucleon interaction for the superfluid gap equation in finite density systems

Masayuki Matsuzaki [a,*], Tomonori Tanigawa [b]

[a] *Department of Physics, Fukuoka University of Education, Munakata, Fukuoka 811-4192, Japan*
[b] *Department of Physics, Kyushu University, Fukuoka 812-8581, Japan*

Received 11 November 1999; revised 1 September 2000; accepted 18 September 2000

Abstract

We construct phenomenologically a relativistic particle–particle channel interaction which suits the gap equation for nuclear matter. This is done by introducing a *density-independent* momentum-cutoff parameter to the relativistic mean field (Hartree and Hartree–Fock) models so as to reproduce the pairing properties obtained by the Bonn-B potential and not to change the saturation property. The interaction so obtained can be used for the relativistic Hartree–Bogoliubov calculation, but some reservation is necessary for the relativistic Hartree–Fock–Bogoliubov calculation. © 2001 Elsevier Science B.V. All rights reserved.

PACS: 21.65.+f; 26.60.+c; 21.60.-n
Keywords: Superfluidity; Nuclear matter; Relativistic mean field

1. Introduction

Pairing correlation between nucleons is a key ingredient to describe the structure of neutron stars and finite nuclei. There are two distinct ways of description of such *finite-density* nuclear many-body systems; the nonrelativistic and the relativistic ones. The latter incorporates the mesons explicitly in addition to the nucleons in terms of a field theory. Both describe the basic properties such as the saturation with a similar quality in different manners. Irrespective of whether nonrelativistic or relativistic, however, various theoretical approaches can be classified into two types: one is realistic studies adopting phenomenological interactions constructed for finite-density systems from the

* Corresponding author.
E-mail addresses: matsuza@fukuoka-edu.ac.jp (M. Matsuzaki), tomo2scp@mbox.nc.kyushu-u.ac.jp (T. Tanigawa).

0375-9474/01/$ – see front matter
PII: S0375-9474(00)00466-8

beginning (hereafter we call this the P-type, indicating "phenomenological"), as often done in the studies of heavy nuclei. And the other is microscopic studies based on bare nucleon–nucleon interactions in free space (the B-type, indicating "bare"). In relativistic studies, typical examples of these two types as for the particle–hole (p–h) channel are the relativistic mean field (RMF) model and the Dirac–Brueckner–Hartree–Fock (DBHF) method, respectively. As for the particle–particle (p–p) channel, that is, pairing correlation, a bare interaction was used as the lowest-order contribution in the gap equation [1] in a study of the B-type [2]. This is thought to be a good approximation at least for the ${}^1S_0$ channel (Refs. [3,4], for example). The first relativistic study of the P-type of pairing correlation in nuclear matter was done by Kucharek and Ring [5]. They adopted a one-boson exchange (OBE) interaction with the coupling constants of the RMF model, which we call the RMF interaction hereafter, aiming at a fully selfconsistent Hartree–Bogoliubov calculation, which we call the P1-type, in the sense that both the p–h and the p–p channel interactions are derived from a common Lagrangian. But the resulting pairing gaps were about three times larger than those accepted in the nonrelativistic studies (see Fig. 6). The reason can be ascribed to the fact that the coupling constants of the RMF model were determined by physics involving only low momenta ($k \leqslant k_{\mathrm{F}}^0$, $\frac{2}{3\pi^2}(k_{\mathrm{F}}^0)^3 = \rho_0$ denoting the saturation density of symmetric nuclear matter), and therefore the adopted OBE interaction is not reliable at high momenta. After a five-year blank, some attempts to improve this were done [6–8]. But their results were insufficient.

An alternative way is to adopt another interaction in the p–p channel while the single-particle states are still given by the RMF model. We call this the P2-type. There are some variations of this. The first one, which we call the P2a-type, adopts another phenomenological interaction for the p–p channel. Actually, the nonrelativistic Gogny force [9] was used combined with the single-particle states of the RMF model for finite nuclei in Ref. [10] and subsequent works, and gave excellent results. The second variation, which we call the P2b-type, is to adopt a bare interaction that describes the high-momentum part realistically, the Bonn potential, again combined with the single-particle states of the RMF model [11,12] (see also Ref. [13]). If one assumes that the RMF model simulates roughly the DBHF calculation, this P2b-type can be regarded as simulating the B-type calculation [2] mentioned above. The results of these P2a- and P2b-types are very similar at densities $\rho < \rho_0$. This supports a statement that the Gogny force resembles a realistic free interaction in the low-density limit [14] (see also Ref. [4]). But a clear difference can be seen at $\rho \sim \rho_0$. This difference can also be seen in fully nonrelativistic calculations; compare the results in Refs. [15,16], for example. The precise origin of this difference has not been understood well. A comparison after taking the polarization effects which have been known to be important at finite densities [17–19] into account may be necessary (see also Ref. [13]). The third variation, which we call the P2b′-type, is to parameterize the p–p channel interaction in terms of a few scattering parameters. This was actually examined by being combined with the DBHF calculation [20], which we call the B′-type (see also Ref. [21]). This method is free from model-dependent ambiguities and meets the viewpoint of modern effective field theories [22,23] but is applicable only to dilute systems. These classifications are summarized in Table 1.

Table 1
Classification of various relativistic approaches to nucleon–nucleon pairing

Type	p–h channel	p–p channel (lowest order)	References
B	DBHF	bare	[2]
B′	DBHF	effective range	[20]
P1	RMF	RMF	[5–8,24]
P2a	RMF	another phenomenological	[5,11,12]
P2b	RMF	bare	[11–13]
P2b′	RMF	effective range	–

Since we are interested in a wide density range where the $^1S_0$ gap exists and would like to respect the selfconsistency in the sense that both the p–h and the p–p channel interactions are derived from a common Lagrangian, here we construct a phenomenological relativistic nucleon–nucleon interaction based on the RMF interaction (the P1-type) by adjusting to the pairing properties given by the RMF + Bonn calculation (the P2b-type). In other words, we aim at constructing an interaction similar to the Gogny force in the sense that it reproduces the pairing properties given by the bare interactions in spite of the fact that it was constructed for the finite-density system from the beginning.

The contents of this paper are as follows: in Section 2 we present our method of constructing a phenomenological p–p channel interaction for the superfluid gap equation. This procedure is applied both to the Hartree and to the Hartree–Fock model. In Section 3, we discuss the pairing properties obtained in the Hartree approximation. Note here that we adopt the no-sea approximation throughout this paper and therefore the relativistic Hartree model means the so-called Relativistic Mean Field model. In Section 4, the relativistic Hartree–Fock–Bogoliubov calculations with or without the modulation of the high-momentum interaction are presented. Conclusions are given in Section 5.

2. Construction of a relativistic particle–particle channel interaction

We start from the ordinary σ–ω model Lagrangian density:

$$\begin{aligned}\mathcal{L} &= \bar{\psi}(\mathrm{i}\gamma_\mu\partial^\mu - M)\psi + \tfrac{1}{2}(\partial_\mu\sigma)(\partial^\mu\sigma) - \tfrac{1}{2}m_\sigma^2\sigma^2 - \tfrac{1}{4}\Omega_{\mu\nu}\Omega^{\mu\nu} + \tfrac{1}{2}m_\omega^2\omega_\mu\omega^\mu \\ &\quad + g_\sigma\bar{\psi}\sigma\psi - g_\omega\bar{\psi}\gamma_\mu\omega^\mu\psi, \\ \Omega_{\mu\nu} &= \partial_\mu\omega_\nu - \partial_\nu\omega_\mu. \end{aligned} \tag{1}$$

The antisymmetrized matrix element of the RMF interaction V derived from this Lagrangian is defined by

$$\bar{v}(\mathbf{p},\mathbf{k}) = \langle \mathbf{p}s', \widetilde{\mathbf{p}s'} | V | \mathbf{k}s, \widetilde{\mathbf{k}s} \rangle - \langle \mathbf{p}s', \widetilde{\mathbf{p}s'} | V | \widetilde{\mathbf{k}s}, \mathbf{k}s \rangle \tag{2}$$

under an instantaneous approximation, with tildes denoting time reversal. After a spin average and an angle integration are performed to project out the S-wave component, its concrete form is given by

$$\bar{v}(p,k) = -\frac{g_\sigma^2}{2E_p^*E_k^*}\left\{1 + \frac{2(E_p^*E_k^* + M^{*2}) - (p^2+k^2+m_\sigma^2)}{4pk}\ln\left(\frac{(p+k)^2+m_\sigma^2}{(p-k)^2+m_\sigma^2}\right)\right\} + \frac{g_\omega^2}{2E_p^*E_k^*pk}\left(2E_p^*E_k^* - M^{*2}\right)\ln\left(\frac{(p+k)^2+m_\omega^2}{(p-k)^2+m_\omega^2}\right),$$

where

$$E_k^* = \sqrt{\mathbf{k}^2 + M^{*2}}. \tag{3}$$

Our policy of constructing a phenomenological interaction proposed above is to introduce a *density-independent* parameter Λ so as not to change the Hartree part with the momentum transfer $\mathbf{q} = 0$ which determines the single-particle energies, respecting that the original parameters of the RMF are density-independent. In the Hartree–Fock model, the $\mathbf{q} \neq 0$ part also contributes to the mean field. This will be discussed in Section 4 in detail. Since the high-momentum part of the RMF interaction does not have a firm experimental basis as mentioned above, we suppose there is room to modify that part. Needless to say, such a modification should be checked by studying independent phenomena, for example, medium-energy heavy-ion collisions. Some adjustments of the density-dependent δ force to the ones that give realistic pairing properties have already been examined in the nonrelativistic studies [4,14]. Among them, a fit to a bare interaction in the $T = 0$ channel was done [4]. We aim at a similar procedure in the relativistic model for the $T = 1$ channel. In the preceding letter [24], the upper bounds of the momentum integration in the gap equation

$$\Delta(p) = -\frac{1}{8\pi^2}\int_0^\infty \bar{v}(p,k)\frac{\Delta(k)}{\sqrt{(E_k - E_{k_\mathrm{F}})^2 + \Delta^2(k)}}k^2\,\mathrm{d}k, \tag{4}$$

where

$$E_k = E_k^* + g_\omega\langle\omega^0\rangle, \tag{5}$$

and the nucleon effective mass equation

$$M^* = M - \frac{g_\sigma^2}{m_\sigma^2}\frac{\gamma}{2\pi^2}\int_0^\infty \frac{M^*}{\sqrt{k^2 + M^{*2}}}v_k^2k^2\,\mathrm{d}k, \tag{6}$$

where the spin–isospin factor $\gamma = 4$ and 2 indicate symmetric nuclear matter and pure neutron matter, respectively, were cut at a finite value Λ, as usually done in condensed-matter physics, since the gap increases monotonically until reaching Kucharek and Ring's value when the model space is enlarged as shown in Fig. 3 of Ref. [8], while $\bar{v}(p,k)$ is left unchanged. We call this method the sudden cutoff hereafter. This was done first in Ref. [5] by inspection. We proposed a quantitative method to determine Λ, which is described below, and obtained 3.60 fm^{-1} for the linear σ–ω parameter set in Ref. [24]. This value almost coincides with their value, about 3.65 fm^{-1}, for the NL2 parameter set.

In the present paper, we examine smooth cutoffs that weaken the high-momentum part; a form factor $f(\mathbf{q}^2)$, $\mathbf{q} = \mathbf{p} - \mathbf{k}$, is applied to each nucleon–meson vertex in $\bar{v}(\mathbf{p},\mathbf{k})$ while

the upper bounds of the integrals are conceptually infinity. They are replaced numerically by a finite number, 20 fm^{-1} which has been proved to be large enough in Ref. [8]. Since there is no decisive reasoning to choose a specific form, we examine four types:

$$\begin{aligned}
\text{monopole:}\quad & f(\mathbf{q}^2) = \frac{\Lambda^2}{\Lambda^2+\mathbf{q}^2},\\
\text{dipole:}\quad & f(\mathbf{q}^2) = \left(\frac{\Lambda^2}{\Lambda^2+\mathbf{q}^2}\right)^2,\\
\text{strong (a):}\quad & f(\mathbf{q}^2) = \frac{\Lambda^2-\mathbf{q}^2}{\Lambda^2+\mathbf{q}^2},\\
\text{strong (b):}\quad & f(\mathbf{q}^2) = \frac{\Lambda^2-m_i^2}{\Lambda^2+\mathbf{q}^2} \quad (i=\sigma,\omega).
\end{aligned} \tag{7}$$

Note that the sudden cutoff above was applied to $\mathbf{k}$, not to $\mathbf{q}$.

The parameter Λ is determined so as to minimize the difference in the pairing properties from the results of the P2b-type RMF + Bonn calculation. Assuming the P2b-type roughly simulates the B-type as mentioned in Section 1, conceptually we aim at fitting to the pairing properties given by the fully microscopic B-type calculation. Here we adopt the Bonn-B potential because this has a moderate property among the available (charge-independent) versions A, B, and C [25]. The pair wave function,

$$\phi(k) = \frac{1}{2}\frac{\Delta(k)}{E_{\rm qp}(k)}, \quad E_{\rm qp}(k) = \sqrt{(E_k - E_{k_{\rm F}})^2 + \Delta^2(k)}, \tag{8}$$

is related to the gap at the Fermi surface,

$$\Delta(k_{\rm F}) = -\frac{1}{4\pi^2}\int_0^\infty \bar{v}(k_{\rm F},k)\phi(k)k^2\,{\rm d}k, \tag{9}$$

and its derivative determines the coherence length [26],

$$\xi = \left(\frac{\displaystyle\int_0^\infty \left|\frac{{\rm d}\phi}{{\rm d}k}\right|^2 k^2\,{\rm d}k}{\displaystyle\int_0^\infty |\phi|^2 k^2\,{\rm d}k}\right)^{\frac{1}{2}}, \tag{10}$$

which measures the spatial size of the Cooper pairs. These expressions indicate that $\Delta(k_{\rm F})$ and ξ carry independent information, ϕ and ${\rm d}\phi/{\rm d}k$, respectively, in strongly-coupled systems, whereas they are intimately related to each other in weakly-coupled ones. Therefore we search for Λ which minimizes

$$\chi^2 = \frac{1}{2N}\sum_{k_{\rm F}}\left\{\left(\frac{\Delta(k_{\rm F})_{\rm RMF}-\Delta(k_{\rm F})_{\rm Bonn}}{\Delta(k_{\rm F})_{\rm Bonn}}\right)^2 + \left(\frac{\xi_{\rm RMF}-\xi_{\rm Bonn}}{\xi_{\rm Bonn}}\right)^2\right\}, \tag{11}$$

where the subscripts "RMF" and "Bonn" denote the RMF interaction including Λ and the Bonn-B potential, respectively, while the single-particle states are determined by the original RMF model in both cases.

The actual numerical task is to solve the gap equation (4) and the effective mass equation for the nucleon (6). They couple to each other through Eq. (5) and

$$v_k^2 = \frac{1}{2}\left(1 - \frac{E_k - E_{k_\mathrm{F}}}{\sqrt{(E_k - E_{k_\mathrm{F}})^2 + \Delta^2(k)}}\right). \tag{12}$$

The parameters of the standard σ–ω model that we adopt are $g_\sigma^2 = 91.64$, $g_\omega^2 = 136.2$, $m_\sigma = 550$ MeV, $m_\omega = 783$ MeV, and $M = 939$ MeV [27]. N in χ^2 is taken to be 11; $k_\mathrm{F} = 0.2, 0.3, \ldots, 1.2$ fm^{-1}. In the following, the results for symmetric nuclear matter are presented. Those for pure neutron matter are very similar except that $\Delta(k_\mathrm{F})$ is a little larger

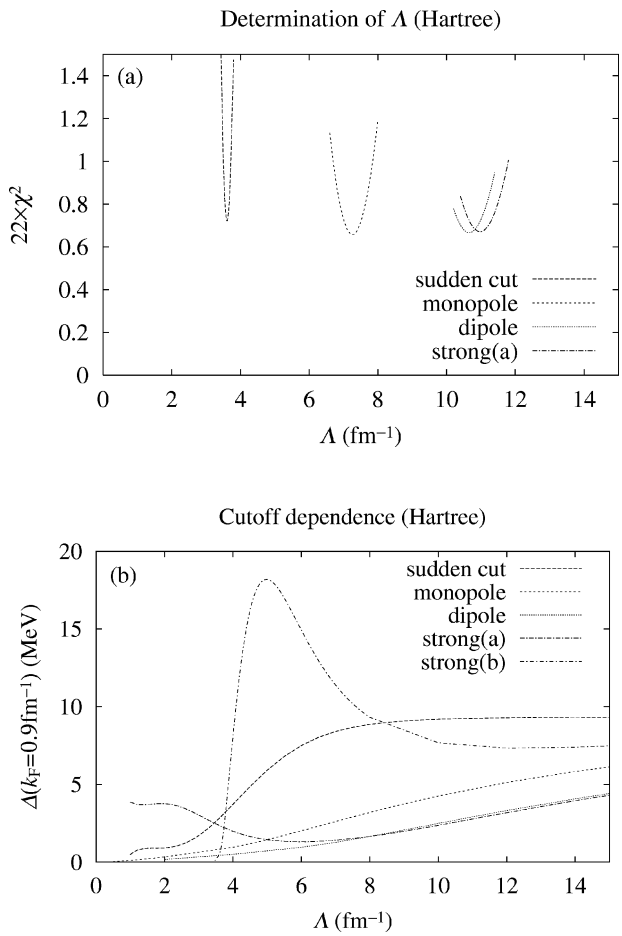

Fig. 1. (a) Curvature of χ^2 in Eq. (11) with respect to the cutoff parameter Λ. (b) Λ-dependence of the pairing gap at the Fermi surface, $k_\mathrm{F} = 0.9$ fm^{-1}. These are the results of the Hartree–Bogoliubov calculation.

due to a larger effective mass M^* as shown in Fig. 1(b) of Ref. [24]. Minimizations of χ^2 give the optimal values, $\Lambda = 7.26$, 10.66, and 10.98 fm^{-1} for the first three types of form factor, respectively, as shown in Fig. 1(a). We do not choose an optimal Λ for the strong (b) type because of its pathological Λ-dependence shown in Fig. 1(b). Fig. 1(b) shows that the Λ-dependence of these smooth cutoff cases is very mild, except for the strong (b) type, in comparison with the sudden cutoff case. The very steep Λ-dependence in the strong (b) case is due to the consecutive depression of the attraction and the repulsion at around $\Lambda \sim m_\sigma$ and $\sim m_\omega$, respectively. In the strong (a) case, although another smaller Λ around 3 fm^{-1} can give similar $\Delta(k_\mathrm{F})$, $\bar{v}(k_\mathrm{F}, k)$ and, consequently, $\Delta(k)$ exhibit an unphysical staggering at around $k \sim m_\sigma$. Therefore we discard this. In addition, although the strong (a) case with $\Lambda = 10.98$ fm^{-1} gives practically the same k_F-dependence of $\Delta(k_\mathrm{F})$ and ξ (in Fig. 2 shown later), $\bar{v}(p, k) = 0$ at $\Lambda = |\mathbf{q}| = |\mathbf{p} - \mathbf{k}|$ brings about an unphysical staggering in $\Delta(k)$ and $\phi(k)$; this leads to an oscillatory structure in r-space with a period $\sim \pi/\Lambda$. Therefore we discard this, too. Form factors with similar Λ are also suggested in a study of medium- energy heavy-ion collisions [28]. This indicates that the present results have a physical meaning.

3. Pairing properties obtained in the relativistic Hartree–Bogoliubov calculation by using the constructed interaction

Fig. 2 presents the results for $\Delta(k_\mathrm{F})$ and ξ as functions of the Fermi momentum k_F, obtained by using the cutoff parameters so determined. Both the monopole and the dipole cases reproduce the results from the Bonn-B potential very well, as the sudden cutoff case studied in Ref. [24], in a wide and physically relevant density range, in the sense that pairing in finite nuclei occurs near the nuclear surface where density is lower than the saturation point [29–31] and that the calculated range of k_F almost corresponds to that of the inner crust of neutron stars [32]. This is our first conclusion. In the present method with a *density-independent* cutoff parameter, some small deviations remain: the overall slight peak shift to higher k_F in $\Delta(k_\mathrm{F})$ and the deviation in ξ at the highest k_F are brought about by the systematic deviation in the critical density where the gap closes, between the calculations adopting bare interactions and those adopting phenomenological ones as mentioned above. The deviation at the lowest k_F is due to the feature that the present model is based on the mean-field picture for the finite-density system; this is a different point from the three-parameter fitting in Refs. [4,14]. Actually, in such an extremely dilute system, the effective-range approximation for free scattering holds well [20].

Next we look into the momentum dependence at $k_\mathrm{F} = 0.9$ fm^{-1}, where $\Delta(k_\mathrm{F})$ becomes almost maximum. Fig. 3(a) shows $\phi(k)$. It is evident that the monopole form factor gives the result identical to the Bonn-potential case as in the sudden cutoff case. This demonstrates clearly the effectiveness of the interaction constructed here. Since we confirmed that the results of the monopole and the dipole cases coincide within the width of the line, hereafter only the monopole case will be shown as a representative. This quantity peaks at $k = k_\mathrm{F}$ as seen from Eq. (8). The width of the peak represents the reciprocal of

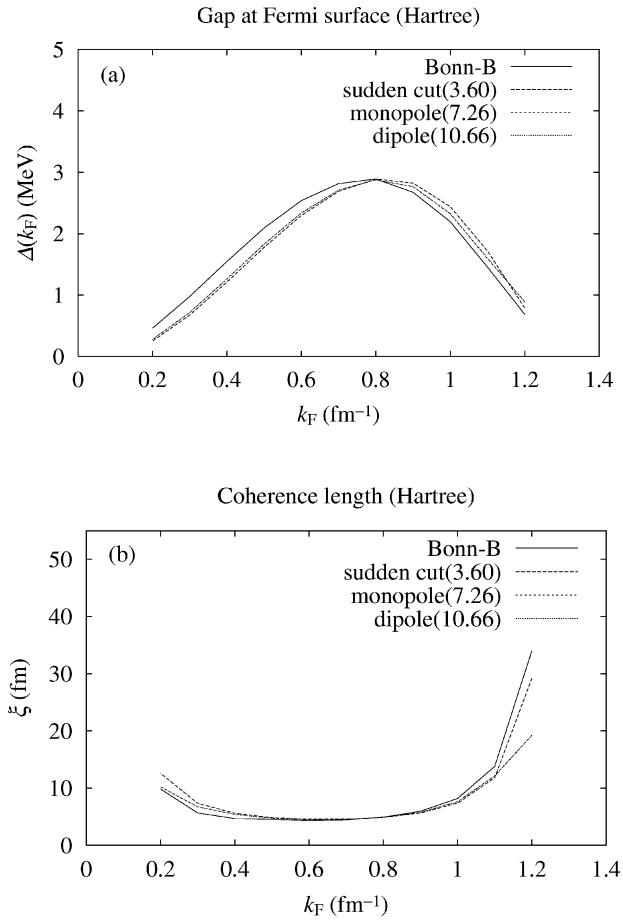

Fig. 2. (a) Pairing gap at the Fermi surface, and (b) coherence length, as functions of the Fermi momentum k_F, obtained by adopting the Bonn-B potential, the sudden cutoff in Ref. [24] and the two types of effective interaction constructed in this study. These are the results of the Hartree–Bogoliubov calculation.

the coherence length. Eq. (8) shows that $\phi(k)$ is composed of $\Delta(k)$ and the quasiparticle energy $E_{qp}(k)$. Fig. 3(b) graphs the former. The gaps of both the sudden cutoff and the monopole form factor cases are almost identical up to $k \sim 2k_F$, and deviations are seen only at larger momenta where $E_{qp}(k)$ are large and accordingly pairing is not important. This is not a trivial result since the bare interaction is more repulsive than the phenomenological ones constructed here even at the momentum region where $\Delta(k)$ are almost identical as shown in Fig. 3(c). The reason why we compare the constructed *p–p channel* interaction with the bare interaction is as follows: although evidently the RMF interaction corresponds to a medium-renormalized one, not to a bare one, here we aim at constructing an interaction similar to the Gogny force in the sense that it reproduces the pairing properties given by the bare interactions in spite of the fact that it was constructed for the finite-density system from the beginning. Accordingly we compare them to see the difference between an

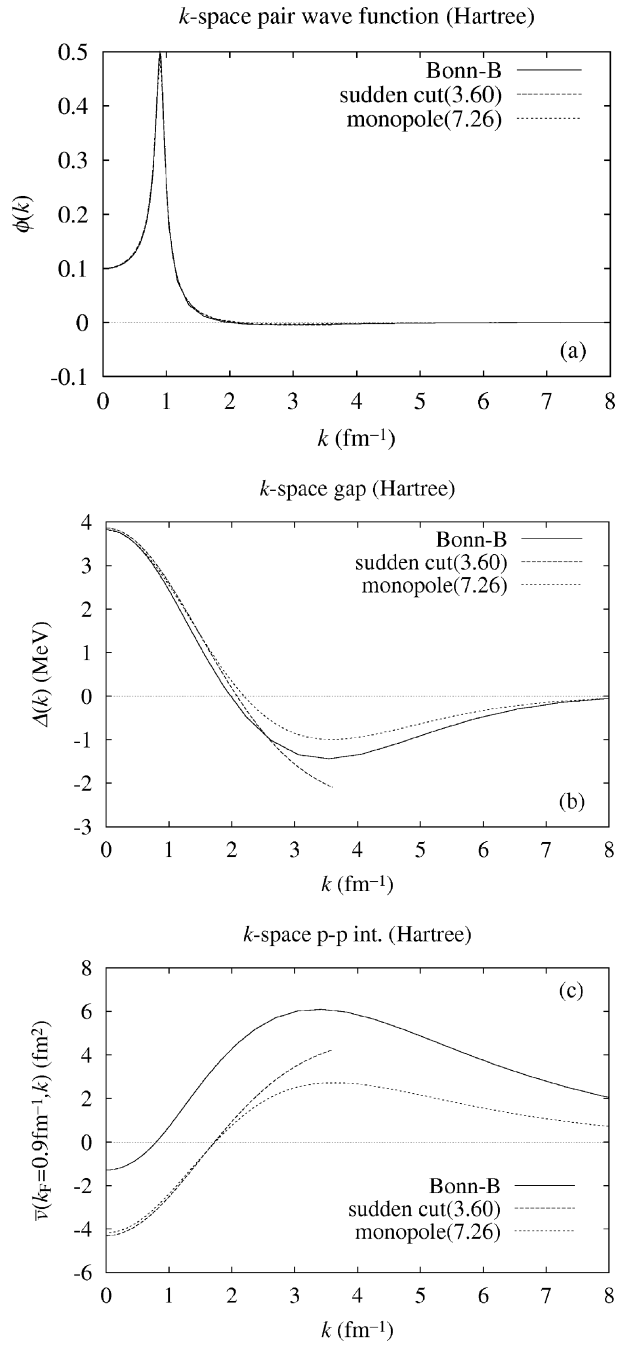

Fig. 3. (a) Pair wave function, (b) pairing gap, and (c) matrix element $\bar{v}(k_{\mathrm{F}}, k)$, as functions of the momentum k, calculated at a Fermi momentum $k_{\mathrm{F}} = 0.9\ \mathrm{fm}^{-1}$, by adopting the Bonn-B potential, the sudden cutoff in Ref. [24] and the effective interaction involving the optimal monopole form factor constructed in this study. These are the results of the Hartree–Bogoliubov calculation.

effective and a bare interactions which give similar pairing properties. This figure indicates that the difference is roughly k-independent.

Here we turn to the dependence on r, the distance between the two nucleons that form a Cooper pair, in order to look into the physical contents further. The gap equation, before the angle integration that results in Eq. (4), can be Fourier-transformed to the local form, $\Delta(\mathbf{r}) = -\bar{v}(\mathbf{r})\phi(\mathbf{r})$ in r-space in the nonrelativistic limit [33]. One can see from this expression that, assuming $\Delta(\mathbf{r})$ is finite, $\phi(\mathbf{r})$ is pushed outwards when $\bar{v}(\mathbf{r})$ has a repulsive core, as the Brueckner wave functions [3,34]. This is related to an observation that the gap equation reduces to a Schrödinger equation for the relative motion of the two particle that form a Cooper pair in the limit of $v_k^2 \to 0$, i.e., at high k [4,35,36]. This, on the other hand,

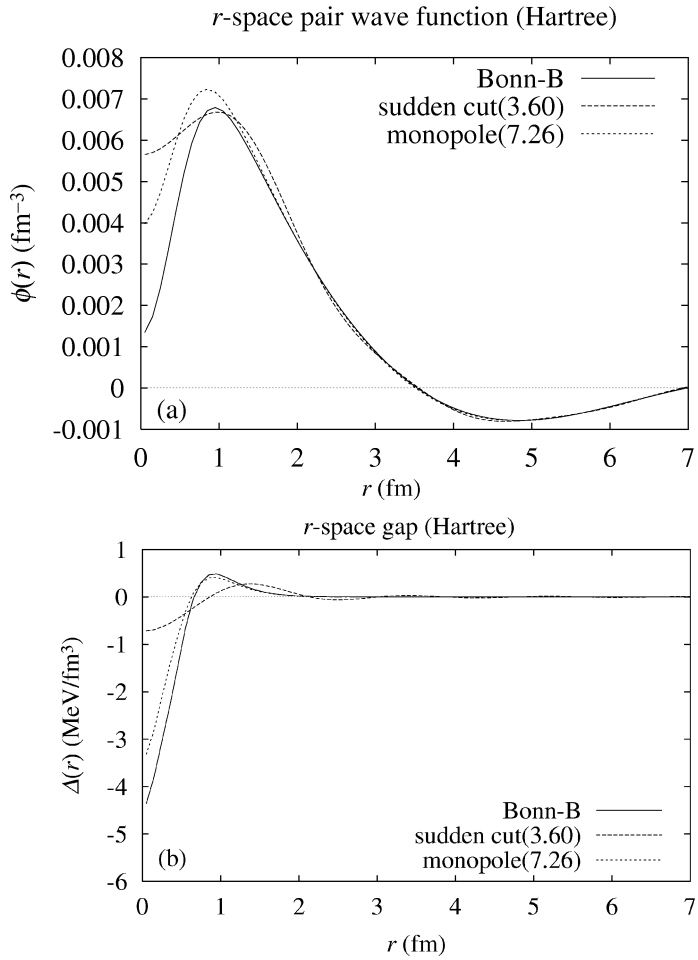

Fig. 4. (a) Pair wave function, and (b) pairing gap, as functions of the distance r, calculated at a Fermi momentum $k_{\mathrm{F}} = 0.9$ fm^{-1}, by adopting the Bonn-B potential, the sudden cutoff in Ref. [24] and the effective interaction involving the optimal monopole form factor constructed in this study. These are the results of the Hartree–Bogoliubov calculation.

masks practically the differences in the repulsive interactions at short range, in other words, widely spread in k-space. The r-space pair wave functions

$$\phi(r) = \frac{1}{2\pi^2} \int_0^\infty \phi(k)\, j_0(kr) k^2 \,\mathrm{d}k, \tag{13}$$

where $j_0(kr)$ is a spherical Bessel function, at $k_\mathrm{F} = 0.9$ fm^{-1} are shown in Fig. 4(a). Appreciable differences are seen only in the core region as mentioned above. The coherence length, that is a typical spatial scale of pairing correlation, is about 6 fm at this k_F as shown in Fig. 2(b); this is almost one order of magnitude larger than the size of the core region. Therefore, practically we can safely use the p–p channel interaction, including the sudden cutoff one, constructed here for the gap equation. Fig. 4(b) shows the corresponding $\Delta(r)$. The gaps are positive at the outside of the core and negative inside in all cases. Note here that the gap equation is invariant with respect to the overall sign inversion; we defined as $\Delta(k_\mathrm{F}) > 0$. Their depths at the inside region reflect the heights of the repulsive core. In the sudden cutoff case, $\Delta(r)$ behaves somewhat differently from others due to the lack of high-momentum components.

4. Relativistic Hartree–Fock–Bogoliubov calculation with a cutoff

In the preceding sections, we have shown that we can construct phenomenologically relativistic p–p channel interactions which give realistic pairing properties by introducing a *density-independent* momentum-cutoff parameter to the (no-sea) relativistic Hartree model. To do this, we have fully utilized the property that only the $\mathbf{q} = 0$ part of the interaction contributes to the Hartree mean field. To see the further applicability of the method presented above, the relativistic Hartree–Fock (RHF) model, in which the $\mathbf{q} \neq 0$ part of the interaction also contributes to the p–h channel, should be examined. In the following, we investigate the relativistic Hartree–Fock–Bogoliubov (RHFB) model with a momentum-cutoff form factor, by comparison with the corresponding Hartree–Bogoliubov calculation. An RHFB calculation with a sudden cutoff was previously done by Guimarães et al. [6]. They obtained very large pairing gaps in the no-sea approximation (Fig. 4 of Ref. [6]). Before studying the effects of the form factor to modulate smoothly the high-momentum interaction, we examine the sudden cutoff — this is a straightforward extension of our previous calculation in Ref. [24] to the RHFB.

The RHF model was described in detail in Refs. [27,37,38], for example. The difference from the Hartree model is the second term in Fig. 5. This introduces the space component of the vector self-energy, Σ^v, and all the Lorentz components of Σ — the scalar Σ^s, the vector (time) Σ^0, and the vector (space) Σ^v — become momentum dependent:

$$\Sigma(p) = \Sigma^\mathrm{s}(p) - \gamma^0 \Sigma^0(p) + \boldsymbol{\gamma} \cdot \mathbf{p} \Sigma^\mathrm{v}(p). \tag{14}$$

In contrast, in the Hartree model, Σ^v is not present, Σ^s and Σ^0 are momentum independent, and Σ^0 is fully determined by the input density. Their concrete forms are

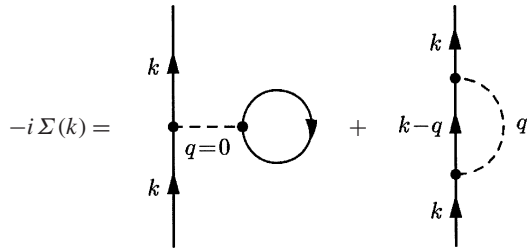

Fig. 5. Feynman diagram representing the nucleon self-energy in the Hartree–Fock model.

$$\Sigma^{\rm s}(p) = -\frac{\gamma}{(2\pi)^3}\frac{g_\sigma^2}{m_\sigma^2}\int_0^{k_{\rm F}} {\rm d}^3k\,\frac{M^*(k)}{E^*(k)}$$
$$+\frac{1}{4\pi^2 k}\int_0^{k_{\rm F}} {\rm d}k\,k\frac{M^*(k)}{E^*(k)}\big[\tfrac{1}{4}g_\sigma^2\Theta_\sigma(p,k) - g_\omega^2\Theta_\omega(p,k)\big],$$
$$\Sigma^0(p) = -\frac{\gamma}{(2\pi)^3}\frac{g_\omega^2}{m_\omega^2}\int_0^{k_{\rm F}} {\rm d}^3k - \frac{1}{4\pi^2 k}\int_0^{k_{\rm F}} {\rm d}k\,k\big[\tfrac{1}{4}g_\sigma^2\Theta_\sigma(p,k) + \tfrac{1}{2}g_\omega^2\Theta_\omega(p,k)\big],$$
$$\Sigma^{\rm v}(p) = -\frac{1}{4\pi^2 k^2}\int_0^{k_{\rm F}} {\rm d}k\,k\frac{k^*}{E^*(k)}\big[\tfrac{1}{2}g_\sigma^2\Phi_\sigma(p,k) + g_\omega^2\Phi_\omega(p,k)\big], \tag{15}$$

with

$$\Theta_i(p,k) = \ln\left|\frac{A_i(p,k)+2pk}{A_i(p,k)-2pk}\right|, \qquad \Phi_i(p,k) = \frac{1}{4pk}A_i(p,k)\Theta_i(p,k) - 1,$$
$$A_i(p,k) = \mathbf{p}^2 + \mathbf{k}^2 + m_i^2 \quad (i=\sigma,\omega), \tag{16}$$

as Eqs. (5.76)–(5.79) in Ref. [27]. The retardation effect is neglected here. Note that the momentum dependence of M^* is stemming from that of $\Sigma^{\rm s}$: $M^* = M + \Sigma^{\rm s}$ (see Eq. (6)). When pairing is introduced, $\int_0^{k_{\rm F}}$ is replaced by $\int_0^\infty v_k^2$, and therefore $\Sigma^{\rm s}(p)$, $\Sigma^0(p)$, $\Sigma^{\rm v}(p)$, and $\Delta(p)$ (Eq. (4)) couple through Eqs. (12) and (5). When the momentum space is discretized to n meshes, these quantities form a set of $4n$-dimensional coupled nonlinear equations; this is a contrast to the $(n+1)$-dimensional ones — $\Delta(p)$ and a momentum-independent M^* or $\Sigma^{\rm s}$ — in the Hartree case.

In order to reproduce the saturation, the coupling constants are adjusted to $g_\sigma^2 = 83.11$, $g_\omega^2 = 108.05$ with the masses being unchanged [27]. We adopt this parameter set for the time being. Other sets will be examined later. Note that the pairing contribution to the energy density around the saturation point is negligible. First we compare the gap at the Fermi surface calculated without a cutoff in RHFB and RHB, in Fig. 6. We call them the full calculations hereafter. The calculated gaps in the former are larger than those in the latter, by about 4 MeV at the maximum, for example. This difference is brought about by that in the coupling constants rather than the Fock effect itself [39]. Actually we confirmed that a Hartree calculation with the coupling constants of the Hartree–Fock gave almost the

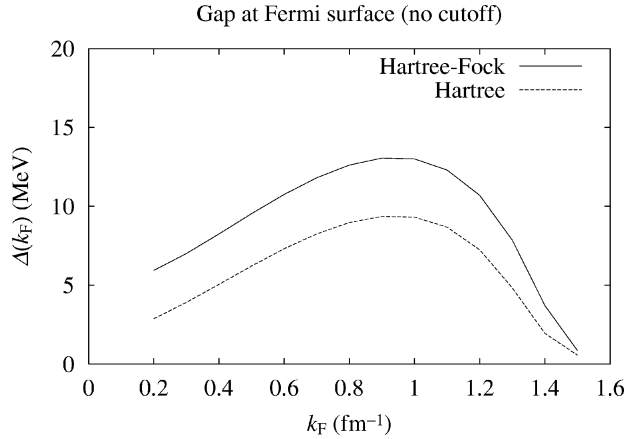

Fig. 6. Pairing gap at the Fermi surface as a function of the Fermi momentum k_F, obtained by the Hartree–Fock–Bogoliubov and the Hartree–Bogoliubov calculations with a large enough momentum cutoff, 20 fm^{-1}.

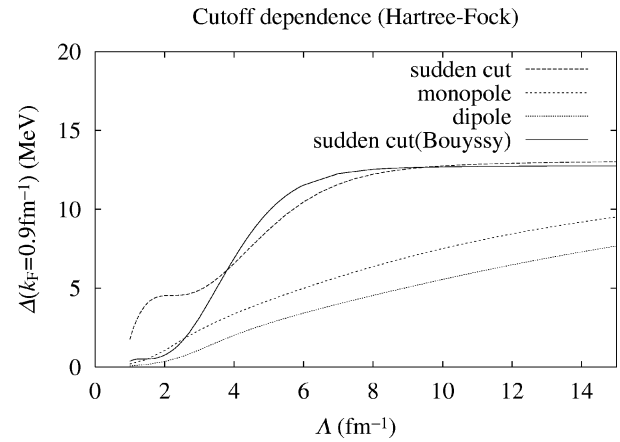

Fig. 7. The same as Fig. 1(b) but for the Hartree–Fock–Bogoliubov calculations.

same gaps as those given by the Hartree–Fock calculation although such a calculation destroys the saturation completely. This result reflects the property that the gap is not sensitive to the detail of the single-particle states. If the coupling constants of Ref. [6], $g_\sigma^2 = 96.392$, $g_\omega^2 = 129.260$ are adopted, calculated gaps become even larger; about 15 MeV at the maximum, for example. But it is evident that this is still smaller than their calculated value in their Fig. 4. The reason for this difference is not clear.

Now let us introduce a sudden cutoff in the upper bound of the momentum integrations in $\Sigma(p)$'s and $\Delta(p)$ as in the previous Hartree case. The result is graphed in Fig. 7 by the long-dashed curve. Although a plateau appears around $\Lambda = 2$ fm^{-1} as in the corresponding case in Fig. 1(b), the gap value of the present plateau is about 4.5 MeV, which is larger than the physical value given by the bare interaction, about 2.8 MeV at this density. Applying the same procedure as in the previous Hartree case, the obtained optimal cutoff is 1.26 fm^{-1}.

This indicates that the attractive interaction alone accounts for the physical magnitude of the gap since the Λ of the plateau corresponds to the k at which $\bar{v}(k_F, k)$ turns from attractive to repulsive [24]. Note that evidently the RHFB calculation with this sudden cutoff can not be applied to the case with $k_F > \Lambda$.

Next we proceed to the smooth cutoff — the form factor in the nucleon–meson vertices. The monopole and the dipole types are examined here. Their Λ-dependence is included in Fig. 7. The optimal cutoffs are $\Lambda = 3.40$ fm^{-1} and 5.02 fm^{-1} for the monopole and the dipole types, respectively. These values are smaller than the corresponding ones in the Hartree cases since the original gap values given by the full calculation are larger. Interestingly, however, their ratio, Λ(monopole)/Λ(dipole), almost coincides with that of

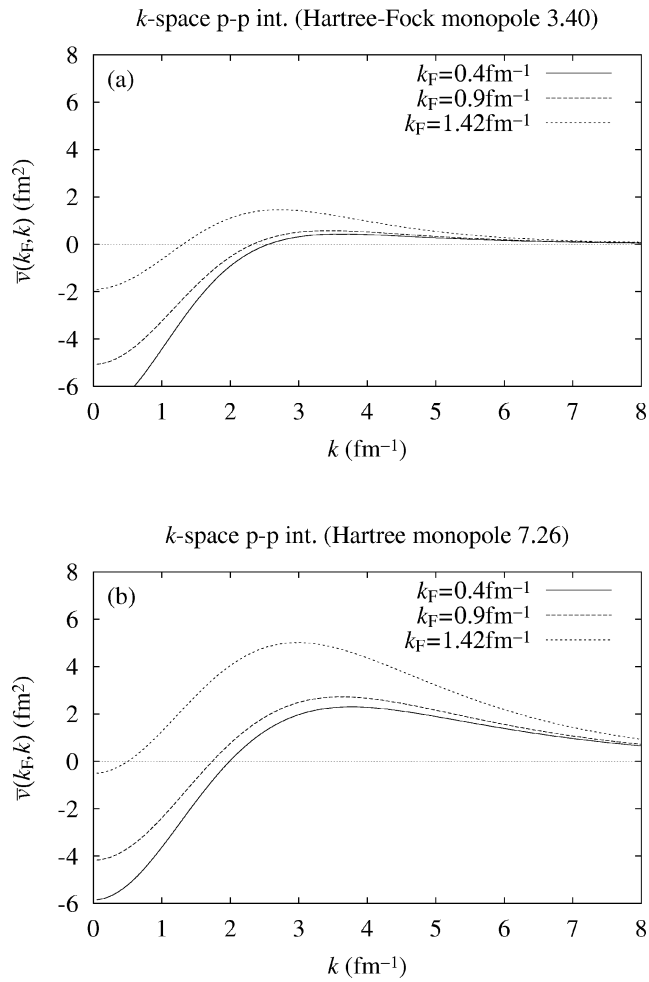

Fig. 8. Matrix element $\bar{v}(k_F, k)$, as a function of the momentum k, obtained by (a) the Hartree–Fock, and (b) the Hartree calculations with the optimal monopole form factors, calculated at three Fermi momenta k_F.

the Hartree case. The p–p channel interactions including the optimal monopole form factor are compared in Fig. 8. The high-momentum repulsive part, in particular at lower densities, is strongly suppressed in the RHFB case. This testifies the discussion about Fig. 7 above that the optimal cutoffs are smaller. In Fig. 9 we present $\Delta(k_F)$ and ξ calculated by adopting the optimal cutoffs. They reproduce the values given by the Bonn-B potential to an extent similar to the Hartree case or a little better except $\Delta(k_F)$ of the sudden cutoff case. Again the results of the monopole and the dipole form factors coincide with each other within the width of the line.

Although the pairing properties of the RHFB with the optimal form factor presented in Fig. 9 are essentially the same as those of the corresponding Hartree calculation, an essential feature of the Hartree–Fock model is that the form factor can affect the saturation property. Therefore we have to check this before concluding the applicability of the present

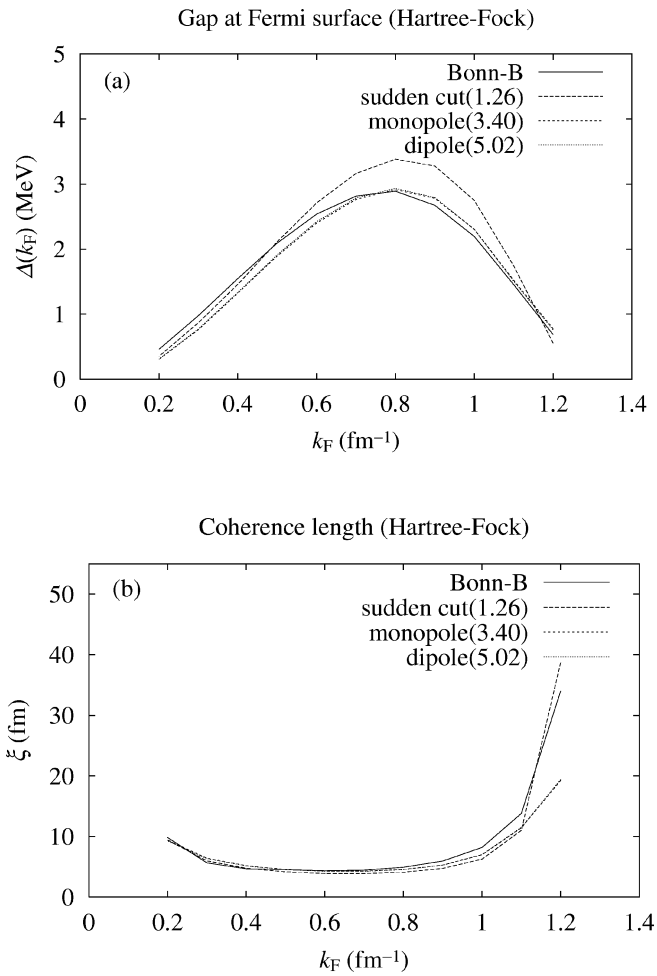

Fig. 9. The same as Fig. 2 but for the Hartree–Fock–Bogoliubov calculations.

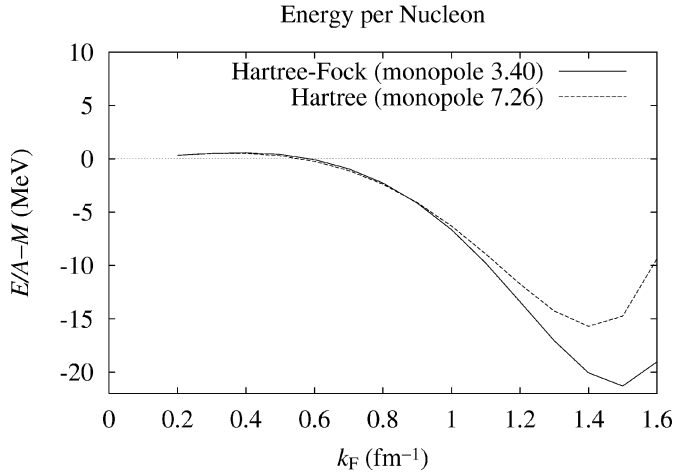

Fig. 10. Energy density including the pairing contributions (both in the Hartree–Fock–Bogoliubov and the Hartree–Bogoliubov calculations) and the cutoff effects (only in the former) as a function of the Fermi momentum k_F.

procedure. The energy density is graphed as a function of the Fermi momentum in Fig. 10. This figure can be compared with Fig. 40 in Ref. [27]. Here the pairing correlation energy (both cases) and the cutoff contribution (Hartree–Fock case only) are additionally included. Although these two curves almost coincide with each other at low densities, the cutoff effect destroys the saturation in the RHFB case. This is because suppressing the high-momentum repulsion breaks the balance between the attraction and the repulsion, and the latter contribute more at higher densities (see Fig. 8(a)). To see this more closely, the cutoff dependence of the energy density without the pairing contribution at the saturation density, $k_F^0 = 1.42$ fm^{-1}, is shown in Fig. 11. In the large-Λ limit, the energy densities approaches to about -15.69 MeV, which is 0.38% less bound than the original value in Ref. [27], -15.75 MeV, because of the instantaneous approximation. This figure shows that

$$\Lambda_{\mathrm{p-p}} < \Lambda_{\mathrm{p-h}}, \tag{17}$$

if we call the cutoff which reproduces the pairing properties and which does the saturation properties $\Lambda_{\mathrm{p-p}}$ and $\Lambda_{\mathrm{p-h}}$, respectively.

Up to now, we used a parameter set of Serot and Walecka. To complete the discussion, other sets with different characteristics are also examined here. One is a set used by Bouyssy et al., $g_\sigma^2 = 69.62$, $g_\omega^2 = 153.81$, $m_\sigma = 440$ MeV, $m_\omega = 783$ MeV, and $M = 938.9$ MeV, which gives saturation at $k_F^0 = 1.30$ fm^{-1} [38]. A distinct feature of this set is that the plateau appears at very small pairing gap (see Fig. 7). This indicates that the repulsive part also contributes to the gap as in the Hartree case, and accordingly, $\Lambda_{\mathrm{p-p}}$ will be larger than in the case of Serot and Walecka's set. Actually, the optimal monopole cutoff is 5.22 fm^{-1}, which is larger than 3.40 fm^{-1} in the previous case. But Fig. 11 shows that still $\Lambda_{\mathrm{p-p}} < \Lambda_{\mathrm{p-h}}$. Another is a set used by Jaminon et al. [37]. An interesting feature of this set is that the saturation (at $k_F^0 = 1.36$ fm^{-1}) is given by introducing a "weak" form factor [40]

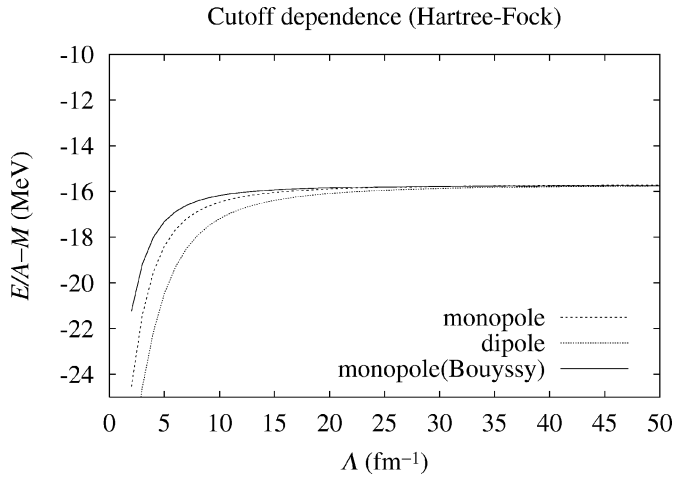

Fig. 11. Energy density at the saturation density corresponding to k_{F}^0 obtained by the Hartree–Fock calculations (without pairing), calculated as a function of the momentum-cutoff parameter in the form factors. $k_{\mathrm{F}}^0 = 1.42$ fm^{-1} for the first two cases, while 1.30 fm^{-1} for the third case. Note that the scale of the abscissa is different from Fig. 7.

$$f(q^2) = \sqrt{\frac{\Lambda^2}{\Lambda^2 - q^2}} \tag{18}$$

from the beginning. Note that here q^2 is the square of the 4-momentum transfer and therefore this contains a retardation effect. The parameters are $g_\sigma^2 = 93.87$, $g_\omega^2 = 127.55$, $m_\sigma = 550$ MeV, $m_\omega = 782.8$ MeV, and $\Lambda = 7.754$ fm^{-1}. Since M is not shown explicitly, 939 MeV is adopted. The RHFB calculation with this form factor under the instantaneous approximation gives pairing gaps which is larger than the physical values; $\Delta(k_{\mathrm{F}}) \simeq 8.5$ MeV at the maximum, for example. This means that still $\Lambda_{\mathrm{p-p}} < \Lambda_{\mathrm{p-h}}$ is necessary to reproduce the physical pairing gap.

In all the calculations above, the cutoff in the form factors is common to σ and ω. Referring to the Bonn potential and Ref. [28], for example, $\Lambda_\sigma \neq \Lambda_\omega$ is another option. Of course large deviations from $\Lambda_\sigma = \Lambda_\omega$ destroy the saturation at least when the coupling constants are kept unchanged. We examined some cases in a limited range, $\Lambda_\omega/\Lambda_\sigma = 0.70$ $(\simeq m_\sigma/m_\omega) - 1.2$, but the results were negative.

5. Conclusions

We have constructed phenomenologically a particle–particle channel interaction which suits the gap equation for nuclear matter. This was done by introducing a density-independent momentum-cutoff parameter to the one-boson exchange interaction derived from the Lagrangian of the RMF model and adjusting it to the pairing properties obtained by the Bonn-B potential. The model pairing properties were calculated by using the RMF model in the p–h channel and the Bonn-B potential in the p–p channel utilizing the

properties that the RMF model simulates crudely [1] the G-matrices in the DBHF calculation and that the pairing properties are not sensitive to the detail of the single-particle states. By this procedure we aimed at constructing an interaction like the Gogny force in the sense that it reproduces the pairing properties given by the bare interactions in spite of the fact that it was constructed for the finite-density system from the beginning. The actual determination of the optimal cutoff parameter was done by the method proposed in our preceding letter for the Hartree mean field plus a sudden cutoff [24].

In the present paper, first we applied this method to the (no-sea) relativistic Hartree model plus various types of form factor which modulates the high-momentum repulsion that spoils the pairing properties. Among the four types examined, the monopole and the dipole form factors exhibit desired properties. Close analyses in momentum space and coordinate space have clarified that the gap equation involves a mechanism to mask the difference in the short-range repulsion between the bare and the in-medium effective interactions and that, in the typical spatial scale of pairing phenomena determined by the coherence length, practically there are no difference in the pairing properties.

Second we performed RHFB calculations with and without a momentum cutoff — a sudden cutoff and two types of form factor. The reason why we examined the RHFB separately is that the form factor which modulates the $\mathbf{q} \neq 0$ part of the interaction also affects the p–h channel. The same procedure was applied; the resulting optimal cutoffs are smaller than those for the Hartree model because the original gap values given by the full calculation without a cutoff are larger. Interestingly, the ratio $\Lambda(\text{monopole})/\Lambda(\text{dipole})$ almost coincides with that for the Hartree model. Having confirmed that these optimal form factors reproduce $\Delta(k_{\mathrm{F}})$ and ξ with a quality similar to that in the Hartree calculation, we looked at the saturation curve of the energy density. Although the results of the RHB and the RHFB each with the optimal form factor coincide with each other up to $k_{\mathrm{F}} \sim 1$ fm^{-1}, the result for the latter starts to deviate at larger k_{F}. This indicates that $\Lambda_{\mathrm{p-p}} < \Lambda_{\mathrm{p-h}}$ is necessary in order also to reproduce the saturation simultaneously using the RMF interaction both in the p–h and the p–p channels. This holds also for the other parameter sets with characteristic features mentioned in the previous section.

These results support the observation that the high-momentum components of the original RMF interaction should be refined. The modulated interaction obtained here by the proposed one-parameter fitting can be successfully used for the relativistic Hartree–Bogoliubov calculation. But its applicability to the relativistic Hartree–Fock–Bogoliubov calculation is limited to low densities.

References

[1] A.B. Migdal, Sov. Phys. JETP 13 (1961) 478.
[2] Ø. Elgarøy, L. Engvik, M. Hjorth-Jensen, E. Osnes, Phys. Rev. Lett. 77 (1996) 1428.
[3] M. Baldo, J. Cugnon, A. Lejeune, U. Lombardo, Nucl. Phys. A 515 (1990) 409.
[4] E. Garrido, P. Sarriguren, E. Moya de Guerra, P. Schuck, Phys. Rev. C 60 (1999) 064312.

[1] The coupling constants must be density-dependent in order to simulate the G-matrices quantitatively.

[5] H. Kucharek, P. Ring, Z. Phys. A 339 (1991) 23.
[6] F.B. Guimarães, B.V. Carlson, T. Frederico, Phys. Rev. C 54 (1996) 2385.
[7] F. Matera, G. Fabbri, A. Dellafiore, Phys. Rev. C 56 (1997) 228.
[8] M. Matsuzaki, Phys. Rev. C 58 (1998) 3407.
[9] J. Dechargé, D. Gogny, Phys. Rev. C 21 (1980) 1568.
[10] T. Gonzalez-Llarena, J.L. Egido, G.A. Lalazissis, P. Ring, Phys. Lett. B 379 (1996) 13.
[11] A. Rummel, P. Ring, Report, 1996.
[12] P. Ring, Prog. Part. Nucl. Phys. 37 (1996) 193.
[13] M. Matsuzaki, T. Tanigawa, Phys. Lett. B 445 (1999) 254.
[14] G.F. Bertsch, H. Esbensen, Ann. Phys. 209 (1991) 327.
[15] R.A. Broglia, F. De Blasio, G. Lazzari, M. Lazzari, P.M. Pizzochero, Phys. Rev. D 50 (1994) 4781.
[16] Ø. Elgarøy, L. Engvik, E. Osnes, F.V. De Blasio, M. Hjorth-Jensen, G. Lazzari, Phys. Rev. D 54 (1996) 1848.
[17] J.M.C. Chen, J.W. Clark, E. Krotscheck, R.A. Smith, Nucl. Phys. A 451 (1986) 509.
[18] J. Wambach, T.L. Ainsworth, D. Pines, Nucl. Phys. A 555 (1993) 128.
[19] H.-J. Schulze, J. Cugnon, A. Lejeune, M. Baldo, U. Lombardo, Phys. Lett. B 375 (1996) 1.
[20] Ø. Elgarøy, M. Hjorth-Jensen, Phys. Rev. C 57 (1998) 1174.
[21] T. Papenbrock, G.F. Bertsch, Phys. Rev. C 59 (1999) 2052.
[22] S. Weinberg, Phys. Lett. B 251 (1990) 288.
[23] B.D. Serot, J.D. Walecka, Int. J. Mod. Phys. E 6 (1997) 515.
[24] T. Tanigawa, M. Matsuzaki, Prog. Theor. Phys. 102 (1999) 897.
[25] R. Machleidt, Adv. Nucl. Phys. 19 (1989) 189.
[26] F.V. De Blasio, M. Hjorth-Jensen, Ø. Elgarøy, L. Engvik, G. Lazzari, M. Baldo, H.-J. Schulze, Phys. Rev. C 56 (1997) 2332.
[27] B.D. Serot, J.D. Walecka, Adv. Nucl. Phys. 16 (1986) 1.
[28] P.K. Sahu, A. Hombach, W. Cassing, M. Effenberger, U. Mosel, Nucl. Phys. A 640 (1998) 493.
[29] M. Baldo, U. Lombardo, E. Saperstein, M. Zverev, Nucl. Phys. A 628 (1998) 503.
[30] F. Barranco, R.A. Broglia, H. Esbensen, E. Viggezzi, Phys. Rev. C 58 (1998) 1257.
[31] M. Farine, P. Schuck, Phys. Lett. B 459 (1999) 444.
[32] T. Takatsuka, R. Tamagaki, Prog. Theor. Phys. Suppl. 112 (1993) 27.
[33] L.N. Cooper, R.L. Mills, A.M. Sessler, Phys. Rev. 114 (1959) 1377.
[34] Ø. Elgarøy, L. Engvik, M. Hjorth-Jensen, E. Osnes, Nucl. Phys. A 604 (1996) 466.
[35] F. Pistolesi, G.C. Strinati, Phys. Rev. B 49 (1994) 6356.
[36] M. Baldo, U. Lombardo, P. Schuck, Phys. Rev. C 52 (1995) 975.
[37] M. Jaminon, C. Mahaux, P. Rochus, Nucl. Phys. A 365 (1981) 371.
[38] A. Bouyssy, J.-F. Mathiot, N. Van Giai, S. Marcos, Phys. Rev. C 36 (1987) 380.
[39] B.V. Carlson, private communication, 1998.
[40] R. Brockmann, Phys. Rev. C 18 (1978) 1510.